Communication

Combustion Synthesis and Characterization of Nanocrystalline WO

Walter Morales, Michael Cason, Olawunmi Aina, Norma R. de Tacconi, and Krishnan Rajeshwar

J. Am. Chem. Soc., **2008**, 130 (20), 6318-6319 • DOI: 10.1021/ja8012402 • Publication Date (Web): 26 April 2008

More About This Article

Additional resources and features associated with this article are available within the HTML version:

- Supporting Information
- Links to the 1 articles that cite this article, as of the time of this article download
- Access to high resolution figures
- Links to articles and content related to this article
- Copyright permission to reproduce figures and/or text from this article

View the Full Text HTML

J|A|C|S
COMMUNICATIONS

Published on Web 04/26/2008

Combustion Synthesis and Characterization of Nanocrystalline WO_3

Walter Morales, Michael Cason, Olawunmi Aina, Norma R. de Tacconi,* and Krishnan Rajeshwar*

Center for Renewable Energy Science and Technology (CREST), Department of Chemistry & Biochemistry, The University of Texas at Arlington, Arlington, Texas 76019-0065

Received February 19, 2008; E-mail: rajeshwar@uta.edu; ntacconi@uta.edu

The energy payback time associated with the semiconductor active material is an important parameter in a photovoltaic solar cell device. Thus lowering the energy requirements for the semiconductor synthesis step or making it more energy-efficient is critical toward making the overall device economics more competitive relative to other nonpolluting energy options. In this communication, combustion synthesis is demonstrated to be a versatile and energy-efficient method for preparing inorganic oxide semiconductors such as tungsten trioxide (WO_3) for photovoltaic or photocatalytic solar energy conversion. The energy efficiency of combustion synthesis accrues from the fact that high process temperatures are *self-sustained* by the exothermicity of the combustion process, and the only *external* thermal energy input needed is for dehydration of the fuel/oxidizer precursor mixture and bringing it to ignition. Importantly, we show that, in this approach, it is also possible to tune the optical characteristics of the oxide semiconductor (i.e., shift its response toward the visible range of the electromagnetic spectrum) in situ by doping the host semiconductor during the formative stage itself. As a bonus, the resultant material shows enhanced surface properties such as markedly improved organic dye uptake relative to benchmark samples obtained from commercial sources. Finally, this synthesis approach requires only very simple equipment, a feature that it shares with other "mild" inorganic semiconductor synthesis routes such as sol−gel chemistry, chemical bath deposition, and electrodeposition.

Oxide semiconductors are eminently attractive candidates for solar energy conversion applications, particularly as photocatalysts for H_2 generation from water.[1] Unlike other candidate semiconductors such as GaP, InP, or CdTe, oxides such as WO_3 do not contain precious metals or toxic elements. They are also chemically inert and have exceptional chemical and photoelectrochemical stability in aqueous media over a very wide pH range.[2,3] As pointed out early in the history of study of this material, the lower optical band gap of WO_3 (~2.7−2.8 eV) relative to that of TiO_2 (~3.0−3.2 eV)—a veritable workhorse in the photoelectrochemical water-splitting community—results in a more substantial utilization of the solar spectrum. Using combustion synthesis, we can shift this response even further toward the visible, as elaborated below.

To date, many methods have been deployed to prepare WO_3 in the form of powders, thin films, or colloidal solutions, including, for example, sol−gel chemistry, thermal oxidation of tungsten, thermal or electron beam evaporation, sputtering, spray pyrolysis, pulsed laser deposition, chemical vapor deposition, and electrodeposition.[4] The present study constitutes the first use of combustion synthesis for preparing nanosized particles of WO_3.

The peroxopolytungstic acid chemistry, relevant to chemical and electrochemical synthesis of WO_3, was adapted in the present study to furnish the tungsten precursor "oxidant" in the combustion synthesis mixture contained in a ceramic crucible. Stoichiometric amounts of the fuel (glycine, urea, or thiourea) were used (see Supporting Information).

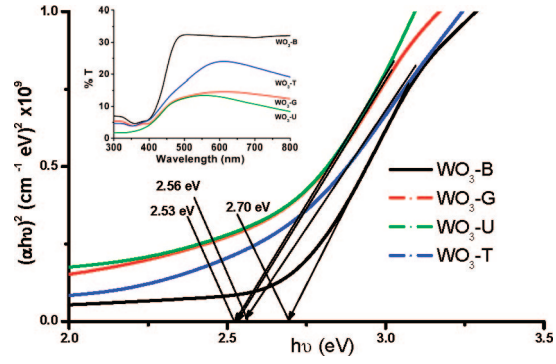

Figure 1. Tauc plots for four WO_3 samples (B, G, U, and T) obtained for the diffuse reflectance data shown in the inset.

The first inkling that the optical response of the combustion-synthesized products are different from the commercial WO_3 sample is furnished by their visual appearance which are markedly darker than the yellow hue of the commercial WO_3 powder. This is quantitatively borne out by the diffuse reflectance UV−visible spectrophotometric data (Figure 1). The spectra in Figure 1a show stronger absorption at wavelengths longer than the bandedge cutoff for all the three combustion-synthesized samples (WO_3−G, WO_3−U, WO_3−T) relative to the benchmark (commercial) sample (WO_3−B). Tauc plots constructed from these data (Figure 1b) afford estimates of the optical band gap (2.53−2.56 eV) for WO_3−G, WO_3−U, and WO_3−T, which are significantly "red-shifted" from the value (2.70 eV) for WO_3−B.

The origin of this optical response shift was further probed by X-ray powder diffraction (XRD) and X-ray photoelectron spectroscopy (XPS). While all the diffraction peaks for monoclinic WO_3 were faithfully reproduced in the WO_3−G, WO_3−U, and WO_3−T samples relative to WO_3−B, the peaks in the former were significantly broadened (see Supporting Information). The latter trend is diagnostic of both diminution of particle size (see below) as well as the strain induced in the oxide lattice by foreign atom incorporation. Thus the high-resolution XPS data show the expected W and O binding energy signals along with adventitious carbon in all the WO_3 samples included in this study (see Supporting Information). Significantly, however, WO_3−G, WO_3−U, and WO_3−T yielded also signals for *extra* carbon (WO_3−G), nitrogen (WO_3−G, WO_3−U, WO_3−T), and sulfur (WO_3−T) (Supporting Information). Clearly, these elements originate from the organic fuel precursors, and the high temperatures generated during combustion would facilitate their subsequent uptake by the oxide matrix. This doping by nonmetallic elements such as C, N, and S has been shown to result in similar visible-light sensitization of TiO_2.[1] However, combustion synthesis affords a simple and versatile approach for incorporating targeted dopants into an oxide matrix simply by varying the chemical composition of the fuel precursor as shown here.

Scherrer analyses of the XRD data afford estimates of the average WO_3 particle size, ~59 nm for WO_3−B and in the ~22, 16, and 12 nm range for WO_3−G, WO_3−U, and WO_3−T, respectively. These

10.1021/ja8012402 CCC: $40.75

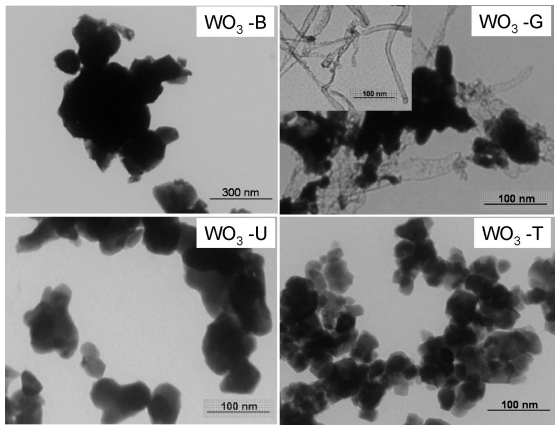

Figure 2. TEM images for WO_3−B, WO_3−G, WO_3−U, and WO_3−T.

estimates are mirrored in transmission electron microscopy (TEM) data which are contained in Figure 2 for selected samples. Clearly, the oxide particles in the combustion-synthesized samples are nanosized (a prerequisite for good photocatalytic activity, see below) but importantly are finer in WO_3−U and WO_3−T relative to WO_3−B (and WO_3−G). This trend is also reflected in the N_2 surface area of the oxide samples (analyzed via the BET model) which (in m^2/g) are 1.74, 1.14, 5.84, and 10.1 for WO_3−B, WO_3−G, WO_3−U, and WO_3−T, respectively.

Methylene blue, a thiazine dye, was used as a probe of the surface and photocatalytic attributes of the combustion-synthesized WO_3 samples relative to the benchmark specimen. This dye is a popular probe in the heterogeneous photocatalysis community, and its "dark" adsorption (on the oxide semiconductor surface) and its subsequent decoloration and decomposition can be monitored via its visible-light absorption signature (at λ_{max} = 660 nm). The data in Figure 3 summarize the important trends. These data were obtained from WO_3 (or TiO_2) dispersions (oxide dose = 2 g/L) equilibrated with the dye in the dark (Figure 3a) or under visible-light illumination (Figure 3b); see experimental details in Supporting Information. Remarkably, ~85 and ~95% of the initial dye was removed from the aqueous solution by adsorption on the WO_3−U and WO_3−T surfaces after 30 min equilibration. Contrastingly, ~84% of the initial dye still *remained in solution* after this same equilibration period for WO_3−B (Figure 3a). More than half of the initial dye has been adsorbed on WO_3−G (Figure 3a), while a commercial Degussa P-25 TiO_2 sample—a popular photocatalyst—shows very little proclivity for dye adsorption even after 24 h (Figure 3a, right side). At least for the WO_3 samples, the above adsorption intensities are in accord with the N_2 surface area trends noted earlier. However, surface chemistry factors are also undoubtedly important as indicated by the fact that the N_2 surface area of Degussa P-25 TiO_2 is ~50 m^2/g; yet its adsorption affinity for the dye is negligible.

Dark adsorption is a prerequisite for good photocatalytic activity,[5] and Figure 3b contains the subsequent temporal evolution of the dye concentration after the excitation visible light is turned on. The data in Figure 3b must be taken to reflect the situation immediately after the adsorption period considered in Figure 3a. Note that the *photocatalytic* decoloration of the dye for WO_3−B and WO_3−G follows

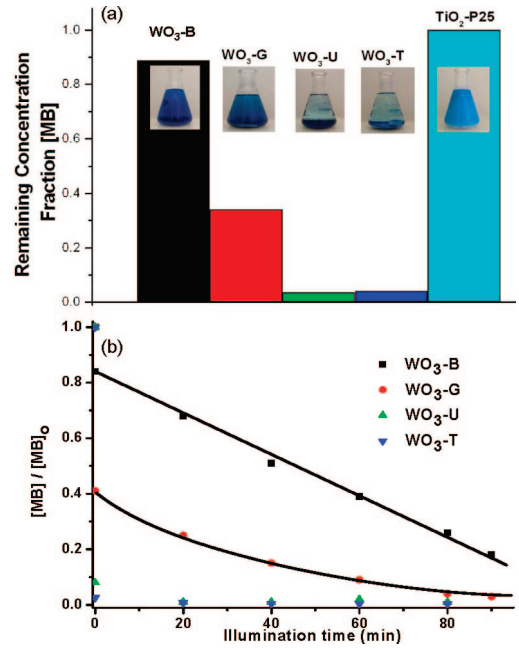

Figure 3. (a) Bar plot showing the remaining methylene blue (MB) in solution equilibrated with 2 g/L of the respective four WO_3 samples and TiO_2 (Degussa P-25) in the dark for 30 min. Pictures of the corresponding dye solutions are inserted for each sample. (b) Subsequent photocatalytic decoloration under visible light for the four WO_3 samples.

zero- and first-order kinetics, respectively, when the light is turned on. The conversion extent for WO_3−U and WO_3−T is already almost complete thanks to extensive initial adsorption of the dye in the dark on the oxide surface.

Further work is in progress to explore the applicability of the combustion-synthesized WO_3 samples in other applications related to photocatalytic and photovoltaic solar energy conversion including experiments with simulated and natural sunlight.

Acknowledgment. This work was supported by the Chemical Sciences, Geosciences, and Biosciences Division, Office of Basic Energy, U.S. Department of Energy. We thank Dr. Willy Lin for assistance with the TEM and BET surface area measurements

Supporting Information Available: Experimental details on the combustion synthesis procedure and the dark adsorption and photocatalysis experiments along with XRD and XPS data. This material is available free of charge via the Internet at http://pubs.acs.org.

References

(1) For example: Rajeshwar, K. *J. Appl. Electrochem.* **2007**, *37*, 765.
(2) Butler, M. A.; Nasby, R. D.; Quinn, R. K. *Solid State Commun.* **1976**, *19*, 1011.
(3) Hodes, G.; Cahen, D.; Manassen, J. *Nature* **1976**, *260*, 312.
(4) Watchenrenwong, A.; Chanmanee, W.; de Tacconi, N. R.; Chenthamarakshan, C. R.; Kajitvichyanukul, K.; Rajeshwar, K. *J. Electroanal. Chem.* **2008**, *612*, 112. See also references cited therein.
(5) For example: Zhao, J.; Wu, K.; Wu, T.; Hidaka, H.; Serpone, N. *J. Chem. Soc., Faraday Trans.* **1998**, *94*, 673.

JA8012402